Lattice and magnetic properties of $ErVO_4$ and $ErPO_4$

Y. Hirano,[1] S. Skanthakumar,[2] C.-K. Loong,[3] N. Wakabayashi,[1] and L. A. Boatner[4]
[1]*Department of Physics, Keio University, Yokohama, Japan 223-8522*
[2]*Chemistry Division, Argonne National Laboratory, Argonne, Illinois 60439*
[3]*Intense Pulsed Neutron Division, Argonne National Laboratory, Argonne, Illinois 60439*
[4]*Solid State Division, Oak Ridge National Laboratory, Oak Ridge, Tennessee 37831*
(Received 16 February 2002; published 17 July 2002)

The crystal-field energy-level structure of the Er^{3+} ground-state multiplet in $ErVO_4$ was investigated by inelastic neutron scattering and magnetic susceptibility methods. The quantitative determination of the crystal-field-level energetics in conjunction with elastic-constant data was used to carry out a detailed analysis of the magnetoelastic contribution to the temperature dependence of the lattice parameters. X-ray-diffraction measurements show that the magnetoelastic effect is small, but the anisotropy with respect to the tetragonal *c* axis is unusual among the rare-earth orthovanadate and orthophosphate series. It was concluded that in $ErVO_4$ the sixth-order multipole contribution is essential for explaining the observed thermal-expansion anomaly. A similar situation also occurs in the case of $ErPO_4$. This result is contrary to the dominating role of the quadrupole effect found previously in many rare-earth orthovanadates and orthophosphates.

DOI: 10.1103/PhysRevB.66.024424 PACS number(s): 75.50.−y, 46.25.Hf

I. INTRODUCTION

Rare-earth orthovanadates, RVO_4, which crystallize in the zircon structure (tetragonal, $Z=4$, space group D_{4h}^{19} *or* $I4_1/amd$ No. 141) throughout the entire rare-earth (R) series (plus $R=$Y and Sc) represent an ideal system for studying the interactions between a sublattice of magnetic ions and the ligands of the host lattice.[1] Each R ion is coordinated by 8 O atoms forming two interpenetrating tetrahedra, each of which is characterized by a unique V-O distance. The point-group symmetry at the R site is D_{2d} $(\bar{4}m2)$. The principal crystal structure can be described as a chain of alternating edge-sharing VO_4 tetrahedra and RO_8 triangular dodecahedra extending parallel to the *c* axis, with the chainjoined laterally by edge-sharing RO_8 dodecahedra. The R ions are expected to retain much of the noninteracting ionic character due to the absence of mediation by conduction electrons in these insulating materials. Therefore, to a first approximation, a single-ion crystal-field (CF) model containing a limited number of parameters may be sufficient to account for the magnetic properties. Any anomalies caused by $4f$ spin-lattice coupling can be recognized through a comparison with the nonmagnetic analogs such as $LaVO_4$ and $LuVO_4$ or with corresponding compounds with R partially replaced by La, Lu, Y, or Sc.

Experimentally, the crystal-field-level structure of R ions in stoichiometric RVO_4 can be determined by neutron spectroscopy based on magnetic scattering.[2] Direct calculations of the CF parameters using various phenomenological models have been attempted by a number of authors.[3–5] However, the results have failed to systematically explain the spectroscopic data. A determination of the CF parameters by first fitting the spectroscopic data and then determining their validity by comparing the calculated and measured magnetic and thermodynamic data remains a practical approach for understanding the basic magnetic properties of these systems. The next level of sophistication is the inclusion of the interactions of the R ions and the host lattice. In this regard, it is useful to examine the properties of the RVO_4 series along with the isostructural families of RPO_4 and $RAsO_4$ compounds since the manifestation of the R spin-lattice interaction varies among different members. In general, coupling of the elastic energy of the magnetic sublattice with the host results in magnetostrictive behavior at temperatures typically below ~ 100 K. Relatively strong anomalies in the temperature dependence of the lattice parameters and/or elastic constants in RPO_4 ($R=$Tb,Dy,Ho,Tm) and RVO_4 ($R=$Pr,Nd,Tb,Dy,Ho,Tm,Yb) were analyzed by a formalism based on the rare-earth quadrupole-lattice strain coupling.[6–11] In this treatment, interactions with the higher-order CF terms were assumed to be negligible. In general, among phosphates and vanadates of the same rare earth, the second-order CF parameters have opposite signs, leading to an opposite anisotropy in the anomalous thermal expansion along the crystallographic *a* and *c* direction. Another type of coupling is a mixing of the CF and phonon states, which may give rise to complex phenomena over a wide range of temperatures. An example of such a case is $YbPO_4$, which exhibits dynamic coupling of the Yb^{3+}:$^2F_{7/2}$ upper CF states with optic phonons, providing evidence of monopolar fluctuations of the Yb orbital.[12,13] Finally, a strong coupling may lead to a cooperative Jahn-Teller transition that results in a transformation of the crystal structure to a lower symmetry in conjunction with magnetic ordering of the R spins, as observed in $TbPO_4$, $TbVO_4$, $TbAsO_4$, $DyVO_4$, $DyAsO_4$, $TmVO_4$, and $TmAsO_4$ at 2.3, 33, 25.5, 13.8, 11.2, 2.2, and 6.1 K, respectively.[14,15]

In the present work, we show that $ErVO_4$ and $ErPO_4$ belong to a category that differs from the aforementioned members in its significantly smaller anomaly in the thermal expansion. There is evidence indicating the same anisotropy in the magnetoelasticity of $ErVO_4$ and $ErPO_4$ in spite of the opposite sign in the second-order CF parameters. Furthermore, the easy-axis direction in the low-temperature magnetic susceptibility of $ErVO_4$ is opposite to that expected

from the sign of the second-order CF parameter.[16] We report the determination of the CF parameters for Er^{3+} ions in $ErVO_4$ by neutron scattering, an analysis of the measured magnetic susceptibility, and a study of the magnetoelasticity by x-ray-diffraction methods. The results of the x-ray measurements for the $ErPO_4$ case will also be presented.

II. EXPERIMENTAL DETAILS

Polycrystalline and single-crystal samples of $ErVO_4$, $ErPO_4$, and $LuVO_4$ were prepared using solution and flux-growth methods, respectively, as described previously.[17,18] The inelastic neutron-scattering experiments were performed using the High-Resolution Medium-Energy Chopper Spectrometer (HRMECS) at the Intense Pulsed Neutron Source (IPNS) of Argonne National Laboratory. Experimental procedures were the same as those described previously in a CF study of $TmPO_4$.[19] The energy resolution (full width at half maximum) of the HRMECS spectrometer varies with energy transfer but is approximately 2–4% of the incident neutron energy (E_0) over the neutron energy-loss spectrum.[20] To explore fully the CF and phonon excitations up to 150 meV, incident energies of 20, 40, 50, and 200 meV were chosen for the measurements at selected temperatures between 7 and 150 K. The magnetic origin of the CF peaks was identified by an examination of the temperature and momentum-transfer dependence of the observed intensities and by comparison with the spectra of the nonmagnetic, isostructural compound $LuVO_4$. The data were corrected for background scattering by subtracting the empty container runs. Measurements of the elastic incoherent scattering from a vanadium standard provided detector calibration and intensity normalization.

A ~3-mg single crystal of $ErVO_4$ was used for the magnetic susceptibility measurements, which were performed using a superconducting quantum intereference device (SQUID) magnetometer over the temperature range of 10–320 K with an applied magnetic field of 500 G. The crystal was mounted on a quartz fiber, and the measurements were made with the applied magnetic-field direction both parallel and perpendicular to the fourfold crystallographic c axis.

The x-ray diffraction experiments on small single crystals of $ErVO_4$ and $ErPO_4$ were carried out at Keio University using a conventional diffractometer with a Cu K_α radiation source. A closed-cycle helium refrigerator was employed for sample cooling. The lattice parameters were determined at selected temperatures between 10 and 300 K by measuring the peak positions of Bragg reflections such as (800), (008), and (107). A difference of less than 10^{-3} Å was generally observed between the lattice parameters of $ErVO_4$ (as well as between those of $ErPO_4$), obtained by x-ray or neutron diffraction.

III. EXPERIMENTAL RESULTS

The Er^{3+}:$^4I_{15/2}$ ground multiplet of $ErVO_4$ is split by the tetragonal CF into 4 Γ_6 and 4 Γ_7 Kramers doublets. As the temperature decreases, the upper CF states are depopulated. Static coupling of the Er low-lying CF states and the crystalline lattice gives rise to magnetoelasticity. This effect manifests itself in an anomalous thermal expansion at low temperatures that was investigated by x-ray diffraction. Variations of the lattice parameters relative to the room-temperature (300 K) values for $ErVO_4$ ($a=7.096$ Å, $c=6.273$ Å) and those for the nonmagnetic reference $LuVO_4$ ($a=7.024$ Å, $c=6.235$ Å) are shown in Fig. 1. The thermal expansion of $ErVO_4$ is highly anisotropic. The difference in the relative change between $ErVO_4$ and $LuVO_4$ at low temperatures is attributed to the magnetoelastic effect in $ErVO_4$. However, compared to the $DyVO_4$ and $HoVO_4$ systems the difference in $ErVO_4$ is 2–3 times smaller. The CF spectra of $ErVO_4$ are shown in Fig. 2. The observed intense peak (labeled A,B at 5 meV) and very weak peaks (C–E) at 7 K correspond to CF excitations from the ground state. At higher temperatures, the intensities of these peaks decrease and other peaks appear due to CF transitions from the populated states. The observed spectra were compared with calculations based on a single-ion model applying the scheme of intermediate coupling and using the spherical-tensor formalism, as employed previously.[16,21,22] Figure 2(c) illustrates the CF level structure of the Er^{3+}:$^4I_{15/2}$ ground multiplet derived from fitting the neutron data. The main difficulty in the fits stems from the very large difference in the intensities of transitions A,B versus C–E (a ratio of ~70:1), which reduces the sensitivity in the differentiation of similar CF parameter sets. The derived CF parameters (set A), given in Table I, reproduce the observed spectra within experimental uncertainty. A comparison of the observed and calculated CF intensities is given in Table II. Table I lists the CF parameters reported in the literature as obtained from optical studies of a dilute analog $Er:YVO_4$,[23] and from magnetic susceptibility measurements[24,25] of single-crystal and polycrystalline samples of $ErVO_4$. During the search for CF parameters by fitting the observed intensities with the CF model using a least-squares method, we identified three other sets of param-

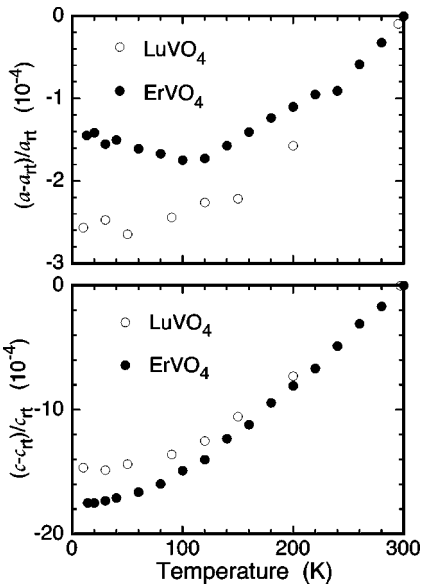

FIG. 1. Changes of the lattice parameters of $ErVO_4$ and $LuVO_4$ relative to the room-temperature values.

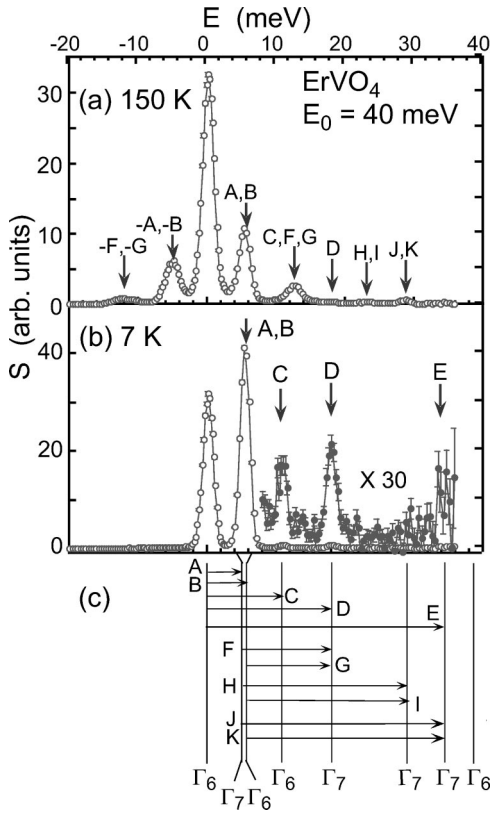

FIG. 2. Observed crystal-field spectra of $ErVO_4$ obtained from neutron inelastic-scattering experiments with an incident energy of 40 meV at 150 K (a) and 7 K (b). (c) The derived Er^{3+}:$^4I_{15/2}$ level scheme. The arrows denote crystal-field transitions (A–J) as observed in the spectra in (a) and (b).

eters that resulted in similar overall chi-square values. Therefore we were not able to declare the uniqueness of parameter set A solely based on the statistical results. However, subsequent examinations of the CF peaks C, D, and E, which show comparable intensities despite of their much lower values than that of the A+B transition, provided a means to differentiate the effects of these parameter sets on the corresponding transition matrix elements. A study of the intensities observed at different incident energies (20, 40, and 50 meV) and temperatures (7, 40, and 100 K), a self-consistency between the experimental data and model prediction can only be achieved with CF parameter A. Therefore we are confident of using parameter set A for all subsequent calculations.

TABLE I. The crystal-field parameters in units of cm^{-1}. Parameter set A was obtained from the present neutron inelastic experiment and was used to calculate the magnetic susceptibility and magnetoelastic contributions to the lattice parameter changes.

	A	B	C	D[a]
B_2^0	−207	−205.6	−186	−157
B_4^0	437	364.0	280	318
B_6^0	−599	−688.0	−702	−656
B_4^4	−834	±925.8	890	−788
B_6^4	159	±31.5	10	121
Refs.	Present work	Kuse *et al.* (Ref. 23)	Chakrabarti *et al.* (Ref. 25)	Guo *et al.* (Ref. 24)

[a]The parameters based on Steven's operator equivalents were converted to spherical tensor representation for comparison.

TABLE II. A comparison of the observed CF intensities with the values calculated from the CF model using parameter set A. The observed and calculated (±A,±B)-peak intensities at 7 K were scaled to the same value. Dependence of the observed intensities on the Boltzmann factor and the Er^{3+} magnetic form factor was included.

CF peaks	Calculated	Observed	Temperature (K)
A,B	100	104±5	7
C	0.192	0.73±0.3	7
D	2.51	1.6±0.3	7
E	2.97	1.69±1	7
A,B	32.5	29±1.5	150
−A,−B	22.5	20±1.6	150
C,F,G	9.23	8.0±1	150
−F,−G	6.26	3.4±0.5	150
E	0.577	1.0±0.5	150
H,I	0.0934	0.52±0.5	150
J,K	4.70	1.6±0.4	150

The calculated magnetic susceptibility of $ErVO_4$ determined using the CF parameters obtained here is compared with the measured susceptibility in Fig. 3, and the agreement is good. These experimental values of the susceptibility, while agreeing well with those obtained by Chakrabarti and co-workers,[25] cover more extensively the temperature range of 10–320 K.

IV. DISCUSSION

The Hamiltonian for magnetoelastic coupling can be written, in the multipole approximation, as linear combinations of products of the strain tensor components and the corresponding CF operators. Here the Steven's operator equivalents[26] are more convenient because of the conformity to expressions in Cartesian coordinates. If only the isotropic and tetragonal components of strains are retained,[8,11]

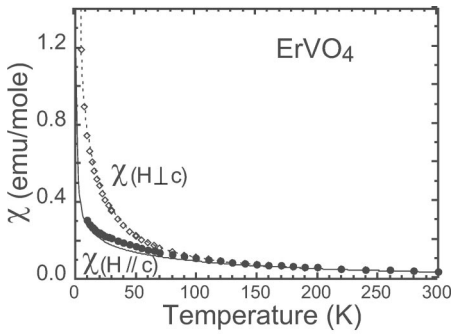

FIG. 3. Measured and calculated magnetic susceptibility of $ErVO_4$.

$$H_{ME} = -\sum_{n=2,4,6} (B_n^{\alpha 1}\varepsilon^{\alpha 1} + B_n^{\alpha 2}\varepsilon^{\alpha 2})\gamma_n O_n^0, \tag{1}$$

where $B_n^{\alpha i}$, $\varepsilon^{\alpha i}$, are the magnetoelastic coefficients and strain components, respectively, and $\gamma_n O_n^0$ are the product of the Steven's factor and operator equivalent. γ_n is related to the reduced matrix elements α_j, β_j, and γ_j of angular momentum j for $n=2,4,6$, respectively.[26] In most rare-earth systems considered in the literature, only the quadrupole O_2^0 was included because of its presumed dominance. However, in the case of $ErVO_4$ and $ErPO_4$, we shall show that the quadrupolar term alone does not account for the magnetoelastic effects on thermal expansion. Instead, the O_6^0 term determines properly the temperature dependence of the lattice parameters.

The magnetoelastic contribution to the thermal expansion is determined from the observed temperature dependences of the lattice constants as

$$\left(\frac{\Delta l}{l}\right)_{ME} \equiv \left[\frac{\Delta l(T)}{l}\right]_{ErVO_4} - \left[\frac{\Delta l(T)}{l}\right]_{LuVO_4}. \tag{2}$$

We assume that the quantity $(\Delta l/l)_{ME}$ is a sum of the contributions from the $(n,0)$-multipolar terms, i.e.,

$$\left(\frac{\Delta l}{l}\right)_{ME} = \sum_n \left(\frac{\Delta l}{l}\right)_{ME}^{(n)}, \tag{3}$$

where

$$\left(\frac{\Delta l}{l}\right)_{ME}^{(n)} = A_n \gamma_n \langle O_n^0(T)\rangle, \tag{4}$$

$$\langle O_n^0(T)\rangle = \frac{1}{Z}\sum \langle \nu|O_n^0|\nu\rangle \exp(-E_\nu/k_B T), \tag{5}$$

and Z is the partition function. The energy of the CF state $|\nu\rangle$ is E_ν. For $ErVO_4$ and $ErPO_4$ it is sufficient to include only the CF states of the ground multiplet because the next multiplet is two orders of magnitude higher in energy.[23] For a tetragonal system, the coefficients A_n for lattice parameters a and c are, respectively,

$$A_n^a = \frac{B_n^{\alpha 1}(C_0^{\alpha 2} + C_0^{\alpha 12}/\sqrt{2}) - B_n^{\alpha 2}(C_0^{\alpha 1}/\sqrt{2} + C_0^{\alpha 12})}{\sqrt{3}[C_0^{\alpha 1}C_0^{\alpha 2} - (C_0^{\alpha 12})^2]}, \tag{6}$$

$$A_n^c = \frac{B_n^{\alpha 1}(C_0^{\alpha 2} - \sqrt{2}C_0^{\alpha 12}) + B_n^{\alpha 2}(\sqrt{2}C_0^{\alpha 1} - C_0^{\alpha 12})}{\sqrt{3}[C_0^{\alpha 1}C_0^{\alpha 2} - (C_0^{\alpha 12})^2]}. \tag{7}$$

$C_0^{\alpha j}$ are symmetrized elastic constants in the absence of magnetic interactions. They are related to the Cartesian elastic constants:

$$C_0^{\alpha 1} = \frac{1}{3}(2C_{11} + 2C_{12} + 4C_{13} + C_{33}), \tag{8}$$

$$C_0^{\alpha 12} = -\frac{\sqrt{2}}{3}(C_{11} + C_{12} - C_{13} - C_{33}), \tag{9}$$

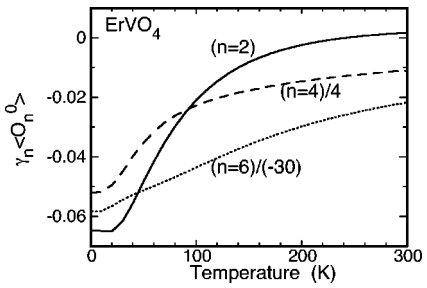

FIG. 4. The calculated temperature dependence of the $(n,0)$ multipoles ($n=2$, 4, and 6) for $ErVO_4$. Values of the fourth- and sixth-order terms were divided by 4 and -30, respectively, in order to display them within the same scale.

$$C_0^{\alpha 2} = \frac{1}{3}(C_{11} + C_{12} - 4C_{13} + 2C_{33}). \tag{10}$$

To proceed with the analysis of the magnetoelastic effects on the lattice parameters, we have to know, with confidence, in addition to the CF parameters, the elastic constants.

The elastic constants were measured by Brillouin scattering techniques using the same $ErVO_4$ single crystals.[27] Since the Brillouin data were obtained at room temperature, the elastic constants are not influenced by the magnetoelastic interactions. In order to confirm the absence of an anomalous temperature dependence of the elastic constants, we monitored the thermal diffuse scattering by x-ray measurements as the sample temperature was lowered below room temperature. The intensity distribution around some Bragg reflections in the $\{hk0\}$ reciprocal-lattice plane were investigated at 300, 120, 40, and 12 K. We found that the pattern of the diffuse scattering distribution remained the same throughout the temperature range while the absolute intensity decreased with decreasing temperature. Therefore phonons in $ErVO_4$ behave normally at low temperatures and the anomalous thermal expansion is not due to the temperature dependence of the phonon frequency.

The temperature dependence of the multipolar terms, calculated according to Eq. (4), is shown in Fig. 4. First, at low temperatures, note the much larger magnitude of the sixth-order term relative to the second-and fourth-order terms. Second, the sixth-order term exhibits a gradual decrease with decreasing temperature throughout the whole temperature range whereas the second- and fourth-order terms drop rapidly and, if scaled, their temperature dependencies are indistinguishable.

It is important to point out the characteristics in the magnetoelastic contribution to the relative change of lattice parameters that are unique to $ErVO_4$. As shown in Fig. 5, the magnitudes of the changes are smaller (by a factor of 2–3) than those of the Dy, Tb, Tm, Pr, and Ho analogs.[28–31] Additionally, the changes along the a and c directions are different by a factor of more than 2 whereas in other RVO_4 members they are comparable. Finally, the anisotropy, $(\Delta a/a)_{ME} > 0$ *and* $(\Delta c/c)_{ME} < 0$ of $ErVO_4$, is opposite to those of other RVO_4 compounds. The lines in Fig. 5 represent the result of a fit to the data using solely the quadrupolar

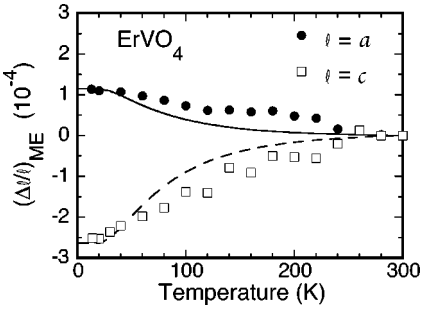

FIG. 5. The observed magnetoelastic effects on the lattice parameters of $ErVO_4$ (symbols) and the corresponding calculated values (lines) assuming only a quadrupole contribution.

contribution. The fit does not follow the temperature dependence of lattice parameter changes over a wide temperature range.

Kazei and co-workers[10,28,29,32,33] have analyzed the magnetoelastic contribution to the thermal expansion of a number of RVO_4 and RPO_4 compounds based on x-ray-diffraction results. The quadrupolar contribution alone was found to be sufficient to explain the data of many compounds. However, in the case of $ErVO_4$ and $ErPO_4$, these authors noted that the quadrupole moment is small and they presented only limited data for $ErPO_4$ with no quantitative analysis for both compounds. Based on the aforementioned remarks on the unique properties of the experimental data and the calculated multipole moments of $ErVO_4$, the present study shows that there is a need to invoke the sixth-order term in the data analysis. Figure 6 shows the result of fitting the data with a linear combination of the second- and sixth-order terms, which reveals a more satisfactory fit throughout the temperature range. As pointed out previously, the temperature dependence of the fourth-order term is nearly identical to that of the second-order term. The resulting coefficients of the fits are given in Table III. It can be seen that A_6^a and A_6^c are about 4–5 times smaller than A_2^a and A_2^c. However, because the value of $\gamma_6\langle O_6^0\rangle$ is about 30 times greater than that of $\gamma_2\langle O_2^0\rangle$ (see Fig. 4), it is the sixth-order term that dominates the magnetoelastic contribution. The coefficients A_6^a and A_6^c, having opposite sign, determine the bifurcation of the thermal-expansion anomaly in $ErVO_4$. The sign of A_2^a is the same to that of A_2^c, and thus, the combined contribution results in significantly different magnitudes of $(\Delta a/a)_{ME}$ and $(\Delta c/c)_{ME}$.

TABLE III. Prefactors and magnetoelastic coefficients obtained from the analysis of thermal-expansion anomaly of $ErVO_4$. The corresponding coefficients for $HoVO_4$ reported by Kazei and co-workers (Ref. 10) are included for comparison. A_n and B_n are in units of 10^{-4} and 10^3 K/f.u., respectively.

	A_2^a	A_2^c	A_6^a	A_6^c	$B_2^{\alpha 1}$	$B_2^{\alpha 2}$	$B_6^{\alpha 1}$	$B_6^{\alpha 2}$
$ErVO_4$	8.5	7.0	1.6	−1.9	3.3	0.16	0.099	−0.32
$HoVO_4$	38	−38			−4.4	6.7		
$ErPO_4$	−19	23	0.96	−1.6				

The A_2^a and A_2^c obtained by Kazei and co-workers[10,32] for other RVO_4 compounds all have the opposite sign and values much larger than the corresponding values of $ErVO_4$ obtained in the present study. Typical values such as those for $HoVO_4$ are included in Table III for comparison. The magnetoelastic coefficients, $B_2^{\alpha 1}$, $B_2^{\alpha 2}$, $B_6^{\alpha 1}$, and $B_6^{\alpha 2}$ for $ErVO_4$ in the units of (K/f.u.), are found to be 3100, 250, 99, and −320, respectively. The constants $B_2^{\alpha 1}$ and $B_2^{\alpha 2}$ for $ErVO_4$ are somewhat smaller in magnitude than those of other RVO_4 and they have the same sign. Moreover, the coefficients $B_6^{\alpha 1}$ and $B_6^{\alpha 2}$ play a decisive role in accounting for the temperature dependence of the lattice parameters caused by magnetoelastic effects.

Due to the relatively large value of $|\gamma_J/\alpha_J|$, the sixth-order term in the crystal-field Hamiltonian has a significant influence in determining the wave functions of the CF states of $ErVO_4$ while the CF parameters are not very different from those of other RVO_4 compounds. The same situation occurs in $ErPO_4$. We performed similar x-ray measurements on $ErPO_4$ and obtained the $(\Delta l/l)_{ME}$ shown in Fig. 7 by the same procedure described previously for $ErVO_4$. As a nonmagnetic reference, the data on $LuPO_4$ were used. The $(n,0)$-multipole moments were calculated using the CF parameters reported previously[16] and shown in Fig. 8. The temperature dependences of the second- and sixth-order terms are not very different down to 50 K. However, the sixth-order term was found to be essential in obtaining a good fit to the experimentally obtained $(\Delta l/l)_{ME}$. It is best fit with a

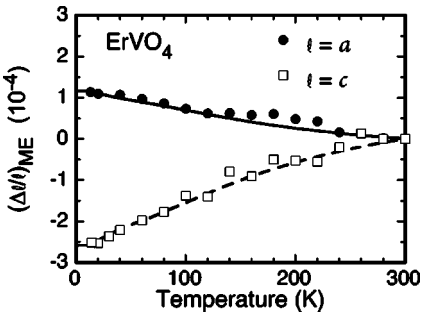

FIG. 6. The observed magnetoelastic effects on the lattice parameters of $ErVO_4$ (symbols) fitted with a linear combination of quadrupole and sixth-order multipole contributions (lines).

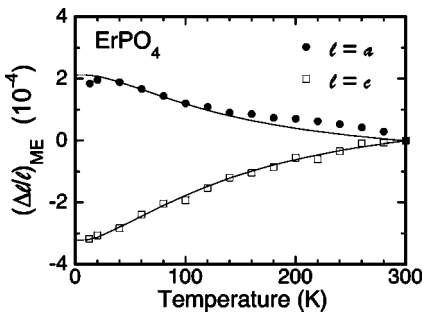

FIG. 7. The observed magnetoelastic effects on the lattice parameters of $ErPO_4$ (symbols) fitted with a linear combination of quadrupole and sixth-order multipole contributions (lines).

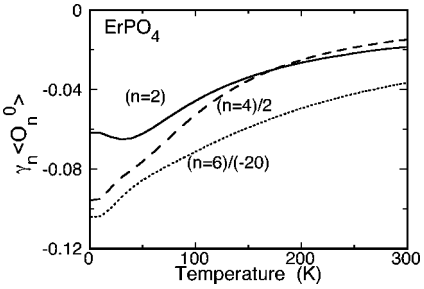

FIG. 8. The calculated temperature dependence of the $(n,0)$ multipoles ($n=2$, 4, and 6) for $ErPO_4$. Values of the fourth- and sixth-order terms were divided by 2 and -20, respectively, in order to display them within the same scale.

linear combination of the second- and sixth-order terms, and the result of that fit is shown as the lines in Fig. 7. The coefficients of the fit are listed in Table III. The fraction of the contribution from the second- and sixth-order terms is comparable to that of $ErVO_4$.

V. CONCLUSION

The zircon-structure RPO_4 and RVO_4 compounds constitute a model system that is ideal for systematic investigations of $4f$ spin-lattice interactions without the complication of conduction-electron mediation. Throughout the rare-earth series, the varying strength of coupling gives rise to different phenomena, from the subtle effect of an anomaly in the thermal expansion to distinct cooperative Jahn-Teller phase transitions and magnetic ordering. Each category requires detailed measurements of the magnetic and thermodynamic properties and data analysis. In the case of $ErVO_4$, we find that it is necessary to validate the CF parameters by an analysis of neutron-scattering and susceptibility data, to independently determine the elastic constants, and assess the phonon contribution at low temperatures by monitoring the thermal diffuse scattering. We concluded that $ErVO_4$ exhibits a small but highly anisotropic thermal-expansion anomaly $[(\Delta a/a)_{ME}>0$ and $(\Delta c/c)_{ME}<0]$ that is opposite to those observed in other RVO_4 members. It is the sixth-order multipole rather than the quadrupole interaction that decides the magnetoelasticity of $ErVO_4$. $ErVO_4$ and $ErPO_4$ are apparently the only rare-earth compounds showing a dominant sixth-order multipolar magnetoelastic contribution. It is interesting to note the unique property of $ErVO_4$ and $ErPO_4$ by comparing this result with the thermal-expansion anomalies in the Pr, Nd, Tb, Dy, Ho, and Tm vanadates and phosphates where the quadrupole term was shown to be the dominant contribution, and with $YbPO_4$ where the Yb monopolelike orbital may couple dynamically with certain phonons. An understanding of the relationship among these phenomena is a challenging task appropriate for future investigations.

ACKNOWLEDGMENTS

Work performed at Argonne National Laboratory and Oak Ridge National Laboratory was supported by the U.S. DOE-BES under contracts No. W-31-109-ENG-38 and No. DE-AC05-00OR22725, respectively. Y.H. gratefully acknowledges financial support from Keio Kougakukai and ANL.

[1] B. C. Chakoumakos, M. M. Abraham, and L. A. Boatner, J. Solid State Chem. **109**, 197 (1994).
[2] C.-K. Loong and L. Soderholm, J. Alloys Compd. **207-208**, 153 (1994).
[3] Vishwamittar and S. P. Puri, Phys. Rev. B **9**, 4673 (1974).
[4] D. J. Newman and G. E. Stedman, J. Phys. Chem. Solids **32**, 535 (1971).
[5] D. Kuse and C. K. Jørgensen, Chem. Phys. Lett. **1**, 314 (1967).
[6] M. D. Kaplan, Phys. Status Solidi B **112**, 351 (1982).
[7] L. Bonsall and R. L. Melcher, Phys. Rev. B **14**, 1128 (1976).
[8] P. Morin, J. Rouchy, and D. Schmitt, Phys. Rev. B **37**, 5401 (1988).
[9] P. Morin, J. Rouchy, and Z. Kazei, Phys. Rev. B **51**, 15 103 (1995).
[10] Z. A. Kazei, N. P. Kolmakova, and O. A. Shishkina, Physica B **245**, 164 (1998).
[11] É. d. T. d. Lacheisserie, Ann. Phys. **5**, 267 (1970).
[12] C.-K. Loong, M. Loewenhaupt, J. C. Nipko, M. Braden, and L. A. Boatner, Phys. Rev. B **60**, R12 549 (1999).
[13] P. C. Becker, G. M. Williams, N. M. Edelstein, J. A. Koningstein, L. A. Boatner, and M. M. Abraham, Phys. Rev. B **45**, 5027 (1992).
[14] G. A. Gehring and K. A. Gehring, Rep. Prog. Phys. **38**, 1 (1975).
[15] G. J. Bowden, Aust. J. Phys. **51**, 201 (1998).
[16] C.-K. Loong, L. Soderholm, J. P. Hammonds, M. M. Abraham, L. A. Boatner, and N. M. Edelstein, J. Phys.: Condens. Matter **5**, 5121 (1993).
[17] M. Rappaz, L. A. Boatner, and M. M. Abraham, in *Alternate Nuclear Waste Forms and Interactions in Geologic Media*, edited by L. A. Boatner and G. C. Battle, Jr. (U.S. Department of Energy, Gatlinburg, TN, 1980), p. 170.
[18] M. M. Abraham, L. A. Boatner, G. W. Beall, C. B. Finch, R. J. Floran, P. G. Huray, and M. Rappaz, in *Alternate Nuclear Waste Forms and Interactions in Geologic Media*, (Ref. 17), p. 144.
[19] C.-K. Loong, L. Soderholm, M. M. Abraham, L. A. Boatner, and N. M. Edelstein, J. Chem. Phys. **98**, 4214 (1993).
[20] C.-K. Loong, S. Ikeda, and J. M. Carpenter, Nucl. Instrum. Methods Phys. Res. A **260**, 381 (1987).
[21] W. T. Carnall, G. L. Goodman, K. Rajnak, and R. S. Rana, J. Chem. Phys. **90**, 3443 (1989).
[22] H. M. Crosswhite and H. Crosswhite, J. Opt. Soc. Am. B **1**, 246 (1984).
[23] D. Kuse, Z. Phys. **203**, 49 (1967).
[24] M.-D. Guo, A. T. Aldred, and S.-K. Chan, J. Phys. Chem. Solids **48**, 229 (1987).
[25] P. K. Chakrabarti, D. Neogy, K. N. Chattopadhyay, and B. M. Wanklyn, J. Phys. Chem. Solids **58**, 393 (1997).
[26] K. W. H. Stevens, Proc. Phys. Soc. London, Sect. A **65**, 209 (1952).

[27] Y. Hirano, I. Guedes, M. Grimsditch, C.-K. Loong, N. Wakabayashi, and L. A. Boatner, J. Am. Ceram. Soc. **85**, 1001 (2002).
[28] Z. A. Kazei and N. P. Kolmakova, Zh. Eksp. Teor. Fiz. **109**, 1687 (1996) [JETP **82**, 909 (1996)].
[29] Z. A. Kazei and N. P. Kolmakova, Zh. Eksp. Teor. Fiz. **103**, 316 (1993) [JETP **76**, 172 (1993)].
[30] S. Skanthakumar, C.-K. Loong, L. Soderholm, J. Nipko, J. W. Richardson, Jr., M. M. Abraham, and L. A. Boatner, J. Alloys Compd. **225**, 595 (1995).
[31] S. Skanthakumar, C.-K. Loong, L. Soderholm, J. W. Richardson, Jr., M. M. Abraham, and L. A. Boatner, Phys. Rev. B **51**, 5644 (1995).
[32] Z. A. Kazei and N. P. Kolmakova, Fiz. Tverd. Tela (St. Petersburg) **37**, 1063 (1995) [Sov. Phys. Solid State **37**, 577 (1995)].
[33] V. I. Sokolov, Z. A. Kazei, and N. P. Kolmakova, Physica B **176**, 101 (1992).